

LA-UR-96-3655

CONF-9610170--6

Los Alamos National Laboratory is operated by the University of California for the United States Department of Energy under contract W-7405-ENG-36

TITLE: **THE DYNAMIC INELASTIC RESPONSE OF  
DELAMINATED PLATES**

RECEIVED  
DEC 25 1996  
OSTI

AUTHOR(S): Frank L. Addessio, T-3  
Todd O. Williams, T-3

SUBMITTED TO: *14th Army Symposium on Solid Mechanics, Myrtle Beach, South  
Carolina, October 15-18, 1996*

DISTRIBUTION OF THIS DOCUMENT IS UNLIMITED *ph*

**MASTER**

By acceptance of this article, the publisher recognizes that the U.S. Government retains a nonexclusive, royalty-free license to publish or reproduce the published form of this contribution, or to allow others to do so, for U.S. Government purposes.

The Los Alamos National Laboratory requests that the publisher identify this article as work performed under the auspices of the U.S. Department of Energy.

Los Alamos

Los Alamos National Laboratory  
Los Alamos, New Mexico 87545

## DISCLAIMER

This report was prepared as an account of work sponsored by an agency of the United States Government. Neither the United States Government nor any agency thereof, nor any of their employees, makes any warranty, express or implied, or assumes any legal liability or responsibility for the accuracy, completeness, or usefulness of any information, apparatus, product, or process disclosed, or represents that its use would not infringe privately owned rights. Reference herein to any specific commercial product, process, or service by trade name, trademark, manufacturer, or otherwise does not necessarily constitute or imply its endorsement, recommendation, or favoring by the United States Government or any agency thereof. The views and opinions of authors expressed herein do not necessarily state or reflect those of the United States Government or any agency thereof.

**DISCLAIMER**

**Portions of this document may be illegible  
in electronic image products. Images are  
produced from the best available original  
document.**

**THE DYNAMIC INELASTIC RESPONSE  
OF  
DELAMINATED PLATES**

**Frank L. Addessio  
Todd O. Williams**

T-3 Theoretical Division  
Los Alamos National Laboratory  
Los Alamos, New Mexico 87545

**Abstract**

A generalized theory for laminated plates with delaminations is used to consider the influence of inelastic deformations on the dynamic behavior of composite plates with delaminations. The laminate model is based on a generalized displacement formulation implemented at the layer level. The delamination behavior can be modeled using any general interfacial fracture law: however, for the current work a linear model is employed. The interfacial displacement jumps are expressed in an internally consistent fashion in terms of the fundamental unknown interfacial tractions. The current theory imposes no restrictions on the size, location, distribution, or direction of growth of the delaminations.

The proposed theory is used to consider the inelastic, dynamic response of delaminated plates in cylindrical bending subjected to a ramp and hold type of loading. The individual layers in the current study are assumed to be either titanium or aluminum. The inelastic response of both materials is modeled using the unified viscoplastic theory of Bodner and Partom. It is shown that the presence of both inelastic behavior and delamination can have a significant influence on the plate response. In particular it is shown that these mechanisms are strongly interactive. This result emphasizes the need to consider both mechanisms simultaneously.

**Introduction**

Laminated composite structures have many potential applications in a variety of engineering fields. However, laminated structures are susceptible to delaminations between layers. The presence of delaminations can cause significant degradation of the structural response characteristics, as compared to perfectly bonded structures. Additionally, it must be recognized that history-dependent inelastic deformations evolve in composite plates under many loading situations. Furthermore, these mechanisms can be highly interactive. Therefore, before potential applications of these types of structures can be realized, analytical tools which can accurately predict these effects must be developed and subsequently employed in the design and analysis process.

A wide variety of work has been done considering the static elastic behavior of delaminated structures. Less work has been done considering the dynamic elastic behavior of delaminated plates. Much of this work has employed variations of the virtual crack extension method to predict the behavior of delaminated composite

plates. To date, very little work seems to have been done considering the dynamic behavior of inelastic delaminated plates.

A recently developed formulation that is capable of incorporating any general nonlinear interfacial fracture behavior in an internally consistent fashion and any general inelastic constitutive model is employed to study the dynamic behavior of inelastic delaminated composite plates (Williams and Addessio, 1996a). In general the form of the interfacial constitutive relations are given by

$$\Delta_i = f_i(\Delta_i, t_i)$$

where  $\Delta_i$  are the displacement jumps and  $t_i$  are the interfacial tractions. The plate theory is based on an approximate higher order discrete layer analysis. No assumptions concerning the location, direction of growth, or number of delaminations are made in the theory. This approach has been shown to provide excellent agreement with both exact static elastic solutions and approximate dynamic solutions.

### Formulation

Consider a single layer. It is assumed that the displacement field within this layer is approximated by

$$u_i(x, y, z, t) = V_i^j(x, y, t) \phi^j(z)$$

where  $j = 1, 2, \dots, N$ .  $N$  is the order of the polynomial expansion. The functions  $\phi^j(z)$  are specified functions of the transverse coordinate  $z$  and the  $V_i^j(x, y, t)$  are the associated displacement coefficients. The governing equations for the layer are obtained by substituting the above displacement field into the principle of virtual work

$$\tau_i^j + N_{i\alpha, \alpha}^j - R_i^j + F_i^j = I^{mj} \dot{v}_i^m$$

where  $m, j = 1, 2, \dots, N$ . The corresponding inplane boundary conditions are

$$V_i^j = \text{specified on } \partial\Omega_1$$

$$T_i^j = N_{i\alpha}^j n_\alpha \text{ on } \partial\Omega_2$$

where  $\partial\Omega = \partial\Omega_1 + \partial\Omega_2$  and  $\partial\Omega$  is the plate boundary. Explicit satisfaction of both the continuity of the interfacial tractions and the jump conditions on the interfacial displacements are utilized to couple the equations governing the behavior of different layers to obtain the governing equations for the laminate. These interfacial conditions are given by

$$(V_i^j)^{k+1} - (V_i^N)^k = \Delta_i^k = f_i(\Delta_i^k, \tau_i^k)$$

$$(\tau_i^j)^k + (\tau_i^j)^{k+1} = 0$$

The above results are completely general and the displacement jumps are expressed in a direct and consistent fashion as a function of the fundamental unknowns in the

theory,  $V_i^j$  and  $\tau_i^j$ . Additionally, the interfacial delamination relations can easily incorporate the constraint that the layers cannot interpenetrate.

The above formulation has been carried out in a sufficiently general fashion that any constitutive law for the behavior of the layer or interface may be incorporated and, therefore, any evolution laws for the local effects can be consistently incorporated into the formulation.

The general theory has been implemented in an explicit finite element code. In the code it is assumed that the temporal gradient in the equation of motion is approximated as

$$\dot{v} = \frac{v - v_0}{\Delta t}$$

where  $v_0$  and  $\Delta t$  are the velocity at the preceding time and the time increment, respectively. Also the left hand side of the equation of motion is evaluated at the previous time step. It is noted that the gradient terms are evaluated using the Mean-Value Theorem.

$$\left\langle \frac{\partial \sigma_{ix}}{\partial x} \right\rangle_m \int \Psi^m d\Omega = \sum_n \left( \int \Psi^m \frac{\partial \Psi^n}{\partial x} d\Omega \right) \sigma_{iz}^n$$

Use of these expressions in the definitions of the force resultants,  $N_{i\alpha}^j$  and  $R_i^j$ , then using these results in the governing equations as known forcing terms allows the new velocities for the layers to be determined. The new velocities are used to update the rate-of-deformation tensor using an expression based on the Mean-Value theorem similar to the above expression. The stresses throughout the plates are then updated by substituting the new rate-of-deformation tensor into the constitutive model for the materials within each layer. Once the stresses are computed, the boundary conditions for the plate are updated and the algorithm pursues advancing the velocities at the next time step. This process is continued until the problem is complete. Further details of the dynamic implementation of the theory are given in Williams and Addressio (1996b)

## Results

The above theory is used to consider the dynamic inelastic response of a composite plate with delamination subjected to cylindrical bending. The plate is composed of two lamina. The top lamina is aluminum and the bottom lamina is titanium, Table 1 (Aboudi, 1991).

TABLE 1. Material Properties

	$E$ (GPa)	$\nu$	$D_0$ (s <sup>-1</sup> )	$Z_0$ (MPa)	$Z_1$ (MPa)	$n$	$m$	$\rho$ (gm/cm <sup>3</sup> )
Al	72.4	0.33	10 <sup>4</sup>	340.0	435.0	10.0	300.0	2.7
Ti	120.0	0.34	10 <sup>4</sup>	1000.0	1400.0	1.0	350.0	4.5

The plate is subjected to a ramping half sine load for  $1 \mu\text{s}$  where the peak value changes from 0 to  $q_0 = 1 \text{ GPa}$ . The load is subsequently held at this peak value for  $4 \mu\text{s}$ . A linear interfacial constitutive relation is employed.

$$\Delta = R\tau$$

where  $\tau$  is the appropriate interfacial stress obtained directly from the theory. Four cases are considered. In case 1 it is assumed that the plate is perfectly bonded and that the individual lamina are elastic. In case 2 the plate is perfectly bonded but exhibits inelastic behavior. In case 3 the lamina deforms inelastically and a value of  $R = 0.25$  (for both normal and shear behavior), is used to model the delamination growth. Case 4 is the same as case 3 with  $R = 1.00$ . The inelastic behavior of the lamina is modeled using the unified viscoplastic theory of Bodner and Partom (Aboudi, 1991).

The transverse displacement as a function of time for the four cases is given in Fig. 1. An explanation of the elastic response (case 1) will be presented first. Then the variations induced by the presence of plasticity and delamination in cases 2-4 will then be discussed. The following discussion is based on simple 1D wave propagation arguments. It is noted that the sound speed of both materials is approximately  $0.5 \text{ cm}/\mu\text{s}$ . During the first microsecond the top surface of the laminate is rapidly accelerated by the applied ramp loading. Both the interface and the bottom surface remain at rest. Just before  $1.5 \mu\text{s}$  the maximum wave value has reached the interface causing the interface to deform. At this point there is a reflected wave in the top lamina and a transmitted wave in the bottom lamina. The top surface begins to deform at a relatively constant rate. Just before  $2 \mu\text{s}$  the transmitted and reflected waves reach the outer surfaces of the laminate resulting in reflected waves from these surfaces. This causes a rapid acceleration of the back surface while the top surface experiences a deceleration. During this time the interface deforms at a fairly constant rate. By  $2.5 \mu\text{s}$  the waves which have been reflected from the outer surfaces of the laminate have reached the interface. The top surface of the laminate continues to deform at a slower rate than was observed at the beginning of the hold segment of the loading history. The bottom surface deforms at a constant rate. As a result of the reflected waves reaching the interface, the interface experiences further acceleration of the transverse deformation. The wave reflection/transmission process continues and results in the further acceleration of the top surface and the deceleration of the bottom surface observed at later times.

Comparison of the predicted responses for case 2-4 indicates that the presence of plasticity results in a delay of the onset of the different trends observed in the elastic case. This is due to the fact that the presence of plasticity mitigates or delays the effects of the elastic waves. In general the presence of plasticity results in larger deflections, especially at the top surface. The presence of delamination further delays the onset of these trends. The delamination represents a stronger impedance mismatch than is observed in the perfectly bonded case. This in turn results in stronger reflected waves and weaker transmitted waves from the interface. The stronger reflected waves in the top lamina result in the observed acceleration of the top surface prior to the deceleration observed in the elastic case. As the delamination becomes bigger due to an increased value of  $R$  the impedance becomes larger and the reflected wave effects become stronger. It is also interesting to note that in case

3 the internal wave propagation behavior results in closure of the delamination. As required no interpenetration of the lamina is observed. Consideration of the relative magnitudes of the displacements in the two lamina at the interfaces indicates that displacement jump due to delamination represents as significant portion of the total displacement change from the top to the bottom surfaces of the laminate.

Figure 2 presents the axial stress distribution at the midplane through the thickness of the lamina at  $5 \mu\text{s}$  for cases 1-3. The presence of plasticity in case 2 causes a shift to a higher stress state in the top lamina and to a generally lower stress state in the bottom lamina. The maximum shift in the top lamina is about 15% while in the bottom lamina the shift is almost 30%. The presence of both plasticity and delamination in case 3 results in more dramatic shifts to generally lower stress states than in either case 1 or 2. This shift results in the entire distribution for  $\sigma_{xx}$  in the bottom lamina being negative.

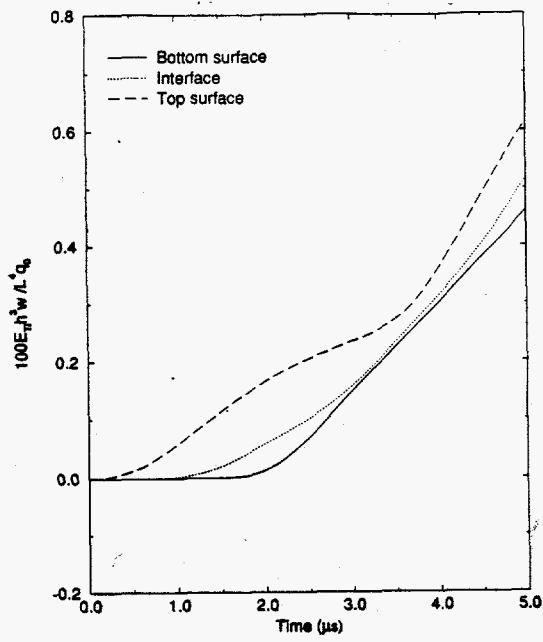
The effective inelastic strain distribution through the thickness of the plate at the midspan is given in Fig. 3 for cases 2 and 3. The presence of the delamination results in a decrease in the peak value of the effective plastic strain at the top surface. However, in general the effective plastic strain is increased through most of the thickness to the top (Al) lamina. The peak value of this increase is about 50%. Alternatively, in the Ti (lower) lamina the effective plastic strain is decreased throughout most of the thickness of the lamina. In fact in the region around the middle of the lamina the value of the effective plastic strain is nearly zero. These changes in the distributions are consistent with the fact that the delamination represents a strong impedance. This impedance maintains stronger wave effects in the top lamina and weak wave effects in the bottom lamina as compared to case 2 where no delamination is present. Thus, the Al (top) lamina experiences higher stresses and therefore undergoes more inelastic deformation while correspondingly the bottom (Ti) lamina supports less inelastic deformation.

In summary, it can be seen that the presence of plasticity and delamination have a significant effect on the behavior of laminated plates.

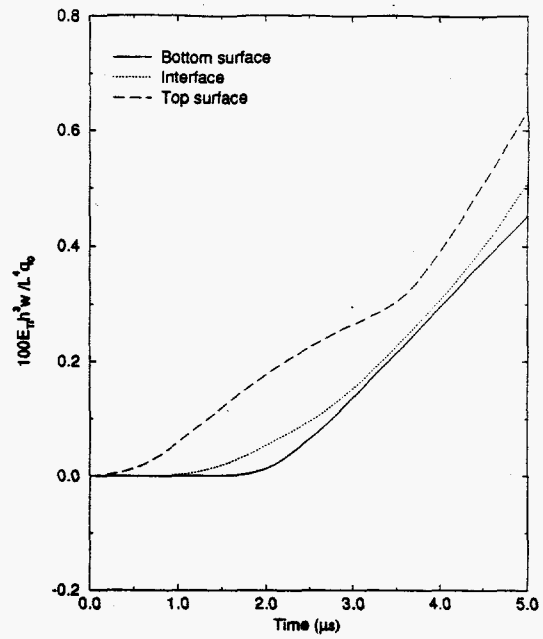
### References

- Aboudi, J. (1991) "The Mechanics of Composite Materials: A Unified Micromechanics Approach", Elsevier Science Publishers B.V., Amsterdam, The Netherlands
- Williams, T.O. and Addessio, F.L. (1996a) "A General Theory for Laminated Plates with Delaminations", *IJSS*, (in press)
- Williams, T.O. and Addessio, F.L. (1996b) "Dynamic Behavior of Laminated Plates with Delaminations", *IJSS*, (in submission)

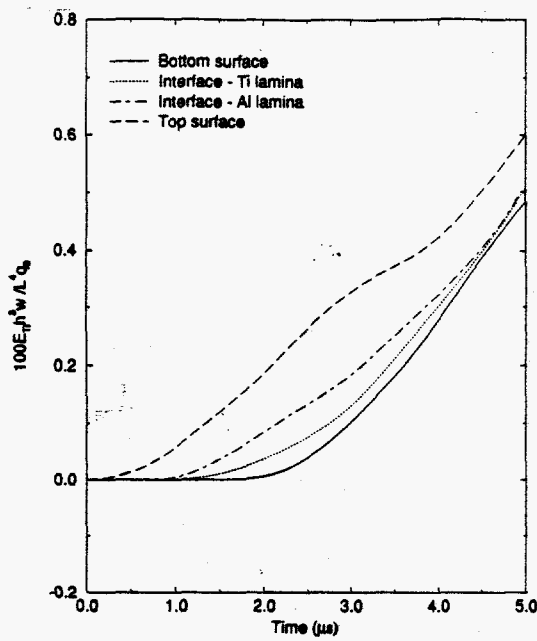




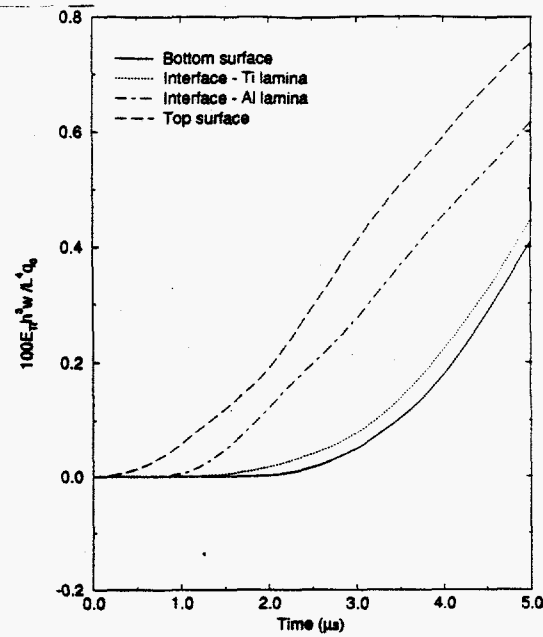
a



b



c



d

Figure 1. Transverse deflection vs. time for a) Case 1, b) Case 2, c) Case 3, d) Case 4.

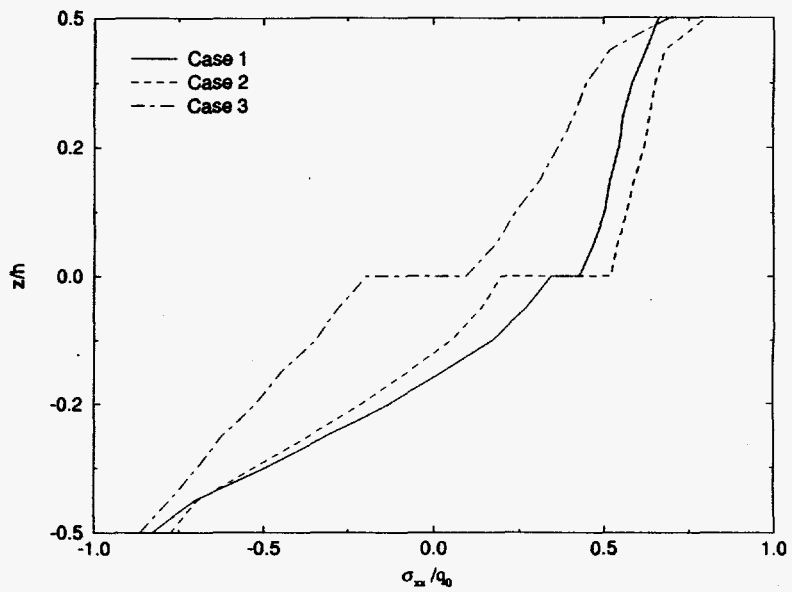


Figure 2. Axial stress distribution at the mid-plane for cases 2 and 3.

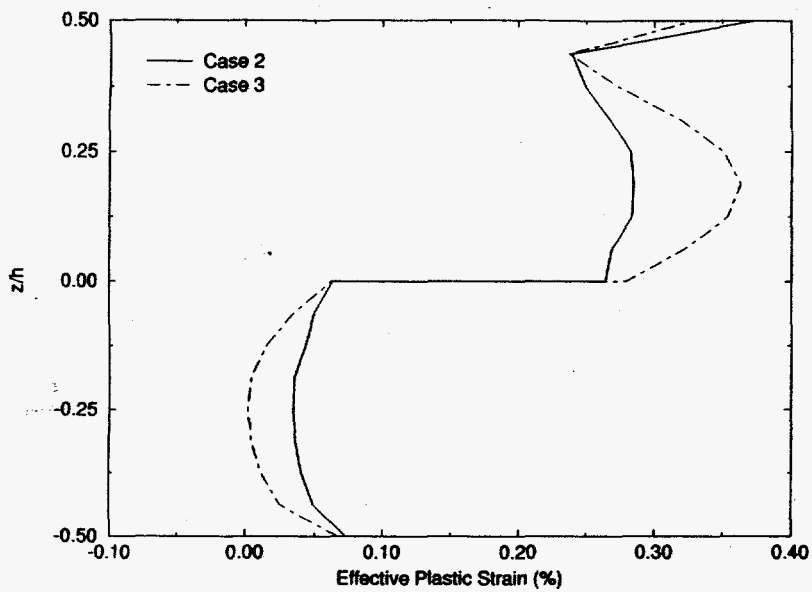


Figure 3. Effective plastic strain distribution at the mid-plane for cases 2 and 3.